SCIENTIFIC REPORTS

OPEN

SUBJECT AREAS:
BIOMECHANICS
HERPETOLOGY
BIOLOGICAL PHYSICS
MECHANICAL PROPERTIES

Received
10 June 2013

Accepted
10 June 2014

Published
27 June 2014

Correspondence and requests for materials should be addressed to M.S. (mspinner@zoologie.uni-kiel.de, sgorb@zoologie.uni-kiel.de)

Subdigital setae of chameleon feet: Friction-enhancing microstructures for a wide range of substrate roughness

Marlene Spinner[1,2], Guido Westhoff[2,3] & Stanislav N. Gorb[1]

[1]Functional Morphology and Biomechanics, Zoological Institute, Kiel University, Am Botanischen Garten 9, 24118 Kiel, Germany, [2]Institute of Zoology, University of Bonn, Poppelsdorfer Schloss, 53115 Bonn, Germany, [3]Tierpark Hagenbeck gGmbH, Lokstedter Grenzstraße 2, 22527 Hamburg, Germany.

Hairy adhesive systems of microscopic setae with triangular flattened tips have evolved convergently in spiders, insects and arboreal lizards. The ventral sides of the feet and tails in chameleons are also covered with setae. However, chameleon setae feature strongly elongated narrow spatulae or fibrous tips. The friction enhancing function of these microstructures has so far only been demonstrated in contact with glass spheres. In the present study, the frictional properties of subdigital setae of *Chamaeleo calyptratus* were measured under normal forces in the physical range on plane substrates having different roughness. We showed that chameleon setae maximize friction on a wide range of substrate roughness. The highest friction was measured on asperities of 1 µm. However, our observations of the climbing ability of *Ch. calyptratus* on rods of different diameters revealed that also claws and grasping feet are additionally responsible for the force generation on various substrates during locomotion.

Hairy adhesive systems have evolved convergently in several animal groups[1,2]. They are present on the extremities of spiders (Arachnida) and insects (Insecta) as well as on toes of several arboreal lizard families[1–5]. Due to their hairy adhesive micro- and nanostructures (setae), the animals are able to walk on smooth inclined or even inverted surfaces without any contributions of their claws.

Comparative studies have revealed that adhesive structures of all clades share a number of common morphological features[1,5–8]. The distal endings of the adhesive setae feature thin terminal plates (spatulae)[1,2,7,9]. Setal length ranges from a few microns to several millimeters[10,11]. Setae of most representatives of the arboreal lizard clades, such as Gekkota, Scincidae and Polychrotidae are not branched, less than 30 µm long, and have triangular spatulae[1,10,12–15]. However, a large number of Gekkota have up to even 110 µm long fourfold branched setae with triangular terminal plates[9,13,16–19].

Despite these similarities in morphology, the mechanism of adhesion is different among animals with hairy adhesives. Whereas many insects secret fluids[20,21] which enhance friction and adhesion by capillary forces[22,23], reptiles feature dry adhesive systems[8]. In reptiles, the best studied adhesive system is that of the Tokay gecko (*Gekko gecko*). Adhesion is based on van der Waals forces, occurring at contacts between spatulae and the substrate[24–26] and is shear-induced[25,27]. In order to maximize friction and adhesion, as many setae as possible should come into contact with the substrate[28]. Spatulae with low thickness make the setae adaptable to various surface profiles[28]. The subdigital microstructures of *G. gecko* feature also asymmetry in their geometry, which is responsible for the force anisotropy during applied shear in proximal and distal directions. Setae are oriented not perpendicular to the epidermal surface, but sloped towards one side[27]. Due to their ability to local deformations, the epidermal structures thereby become adaptable to different surface profiles. In reptiles with non-branched setae, spatulae also project in a certain direction[1,5]. In Gekkota, with multifold branched setae, all the spatulae of one seta are evenly aligned in one plane[9,16,29,30]. Nonetheless, both friction and adhesive forces of the subdigital pads of *G. gecko* are not equally strong on different surface profiles[31,32].

Considering the widespread occurrence of setal adhesive pads in arboreal lizards, it is not surprising that arboreal Chamaeleonidae also have setae on the ventral sides of their feet (subdigital) and tail (subcaudal)[33–36] (Fig. 1 a–c). In the genera *Calumma*, *Chamaeleo*, *Furcifer*, and *Trioceros*, setae are 6–20 µm long[36]. Thus, they have similar dimensions as the non-branched setae of scincid and polychrotid lizards and some Gekkota[1,10,12–15]. In contrast to the adhesive pads of other lizard clades, chamaeleonid setae have no triangular tips, but feature fibrous tips or narrow elongated spatulae that are neither oriented nor inclined, but flexible and bendable in any direction[36]. However, the chamaeleonid system also features differences on the macro scale. Whereas other pad

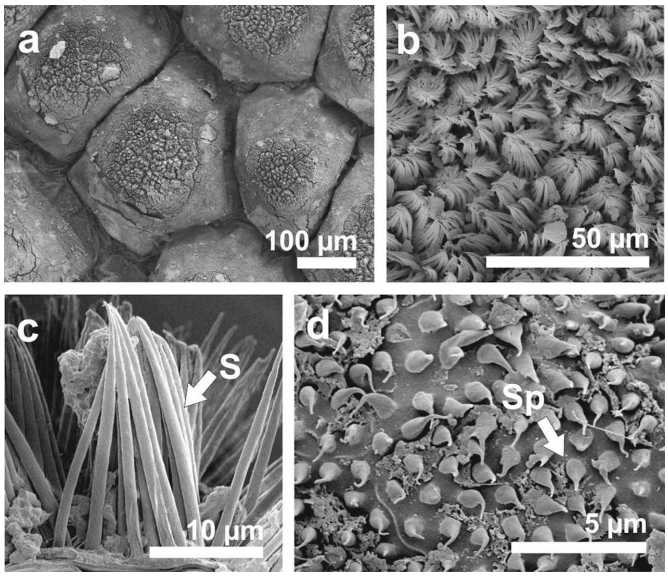

Figure 1 | Scanning electron micrographs of the epidermis of *Chamaeleo calyptratus* (adapted from Spinner et al., 2013). (a) Subdigital scales. (b) The apical surface of a subdigital scale is covered by setae. (c) Cross-section of the apical surface of a subdigital scale. The surface is covered by setae (S). (d) Scales of the dorsal epidermis of the feet of *Ch. calyptratus* are covered by very short seta-like structures called spines (Sp).

bearing lizards are able to splay each of their toes, chamaeleonid toes are merged into pairs and triplets forming grasping feet[37,38]. Also the subdigital surfaces have different shapes. In chameleons, setae cover the apical surfaces of conical subdigital scales[35,36]. In Polychrotidae[12] and Gekkota[17], adhesive setae are located on adhesive lamellae. As in Gekkota and Polychrotidae, the entire body of chameleons from the genera *Calumma*, *Chamaeleo*, *Furcifer*, and *Trioceros* is covered with microscopic protuberances, so-called spines[33–36,39,40] (Fig. 1 d).

Despite the well examined morphology of the microstructure on the feet and tails of chameleons (see references above) and studies on the locomotion of these animals[41,42], there is only one study examining the function of the subdigital microstructure[43]. Sliding friction forces between glass beads of 0.5 and 4 mm and the dorsal and ventral epidermis of the feet of two individuals of *Ch. calyptratus* were measured over a sliding distance of 0.1 and 1 mm under different load conditions (1, 2, 5, 10 and 20 mN)[43]. Under a normal load of 5 mN and above a significant increase of friction of the subdigital epidermis ($\mu = 0.21 \pm 0.06$) in comparison to the dorsal epidermis of the feet ($\mu = 0.1 \pm 0.08$) was found. However, the interaction of chameleon setae with glass beads poorly describes their function on the wide range of natural surfaces. The range of friction that can be generated by the chameleon's hierarchical system of claws, scales, and microstructures remains unclear, since the glass beads and the pulling distance are of similar dimensions to those of conical scales of the *Ch. calyptratus* (diameter about 500 µm) and thereby determine frictional properties only on microscale. Additionally, the normal load applied by grasping movements of living animals on flat substrate is rather homogenously distributed over the entire subdigital surface, whereas in the glass bead experiment contact is restricted to a relatively small area which could cause non-uniform deformation of the scales. However, this situation more corresponds to the natural situation on strongly corrugated substrate.

In this study we test friction properties of the entire setal pads of *Chamaeleo calyptratus* (veiled chameleon) in comparison to the epidermis on the dorsal side of its feet. This species has by far the longest setae (20 µm long) ending in hairy tips[36] (Fig. 1 c). We measured frictional properties of subdigital and dorsal feet epidermis of

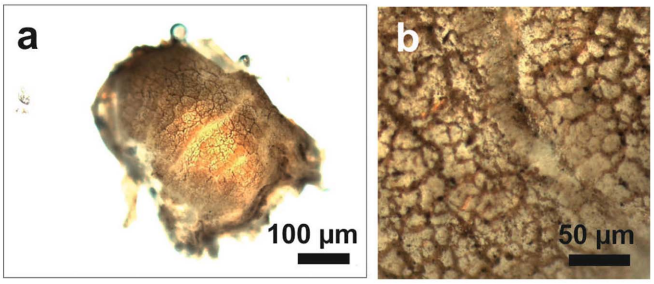

Figure 2 | Subdigital scale of *Chamaeleo calyptratus* in the light microscope. (a) Low magnification. (b) Setae on the scale at the higher magnification.

anesthetized animals on different roughness and compared them. In order to get more data, further frictional measurements were done with the subdigital epidermis of three dead individuals of this species. To gain an insight on how and under which conditions the system of subdigital pads functions in real behavioral situation, we additionally examined the climbing behavior of three individuals of *Ch. calyptratus* under different conditions. Based on the animals' behavioral traits of avoiding slipping with maximal pressure of their grasping feet, we documented the climbing performance of this species on cylinders of different materials, surface roughness and diameter of substrata with increasing inclination. Data from this experiment shed light upon the combined contribution of the muscle power, claw action, and frictional properties of setal pads to the firm grip in real situation during locomotion. Furthermore, these results demonstrate the influence of substrate profile on the chameleon locomotion.

Results

Light microscopy. Our light microscopy images showed that subdigital scales of an exuvia of *Ch. calyptratus* are covered with setae (Fig. 2a) that are arranged in irregular clusters (Fig. 2b).

Frictional measurements. Data of the frictional measurements of surfaces with different roughness as well as ventral and dorsal epidermis (Fig. 3) of the feet of three individuals of *Ch. calyptratus* are presented in Figs. 4–5. Surface parameters of the substrates are listed in Table 1. Once the system was set in relative motion, the friction forces remained approximately constant (dynamic friction). Stick-and-slip events which could be potentially visible in the curve

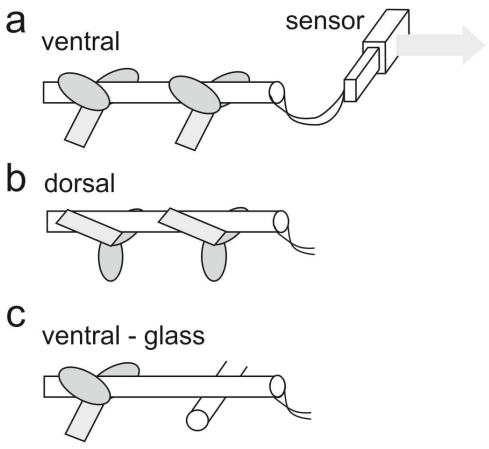

Figure 3 | Draft of the experimental setup for friction measurements. (a) Measurement of the subdigital epidermis. (b) Measurement of the dorsal epidermis of the feet and epidermis of antebrachium. (c) Measurement with one glass support and the subdigital epidermis.

as peaks were not observed (Fig. 4 b). Measurements showed that sliding friction of the cylinder surfaces is about 90% higher on the subdigital epidermis than on the dorsal epidermis of the feet. Comparison of the data of the three living animals shows that the difference is significant for all tested polish papers and under both load conditions (Kruskal-Wallis One Way ANOVA on ranks, $P \leq 0.001$; Pairwise multiple comparison, Tukey Test $P < 0.05$) (Table 2, 3). For example, under a load force of 981 mN on the 12 μm grain size substrate (root-mean-square-roughness (Rq) 4.16 μm), the difference between sliding friction coefficients of the dorsal and ventral epidermis of the feet ($\Delta\mu$) was about 0.36. Only in measurements using the glass cylinder, the differences of frictional properties of ventral and dorsal feet epidermis were not significant and smaller than on polishing papers ($\Delta\mu = 0.084$) (Kruskal-Wallis One Way ANOVA on ranks, $P \leq 0.001$; Pairwise multiple comparison, Tukey Test $P < 0.05$) (Table 3). The Kruskal-Wallis One Way ANOVA on ranks ($P \leq 0.001$) and a Tukey Test ($P < 0.05$) show a significant difference of friction coefficients of subdigital epidermis of the three living individuals at 589 mN normal load on the different substrates (Table 4). Measurements under higher normal load of 981 mN normal load did not lead to significantly different frictional coefficients, but rather showed the same substrate depended variation of friction (Kruskal-Wallis One Way ANOVA on ranks, $P \leq 0.001$; Tukey Test $P < 0.05$, for all substrates) (Table 4). We cannot entirely exclude that the differences in frictional properties on glass and the polish papers are a result of different chemistry of these materials. However, as different polish papers consist of the same material, all significant differences on these substrates can be addressed to the differences of grain size. Subdigital epidermis featured the highest sliding friction coefficient (μs) of 0.87 and 0.73 on the polishing papers having a grain size of 1 μm and 3 μm (Rq = 0.47 μm and Rq = 1.37 μm). Sliding friction coefficients on the polish paper with the grain size of 1 μm were significantly higher than on all other substrates with an exception with the roughness of 3 μm having also a high friction coefficient (Kruskal-Wallis One Way ANOVA on ranks, $P \leq 0.001$; Tukey Test, $P < 0.05$). Although our recorded force-time curves do not allow conclusions about the exact magnitude of static friction, they show that static friction coefficients are slightly lower than sliding friction coefficients. Our plot of sliding friction forces under 177, 569, 589 and 981 mN normal forces showed that on all substrates, both forces are proportional to each other according to the equation $Fs = \mu s\, FN$[44] (see regression lines in Fig. 5).

Friction data were analyzed with a linear mixed-effects model, where individual differences and the different substrate types were considered as random effects and normal forces as fixed effect. Despite friction forces were also influenced by individual variability (standard deviation SD = 35.09) and other undefined random effects

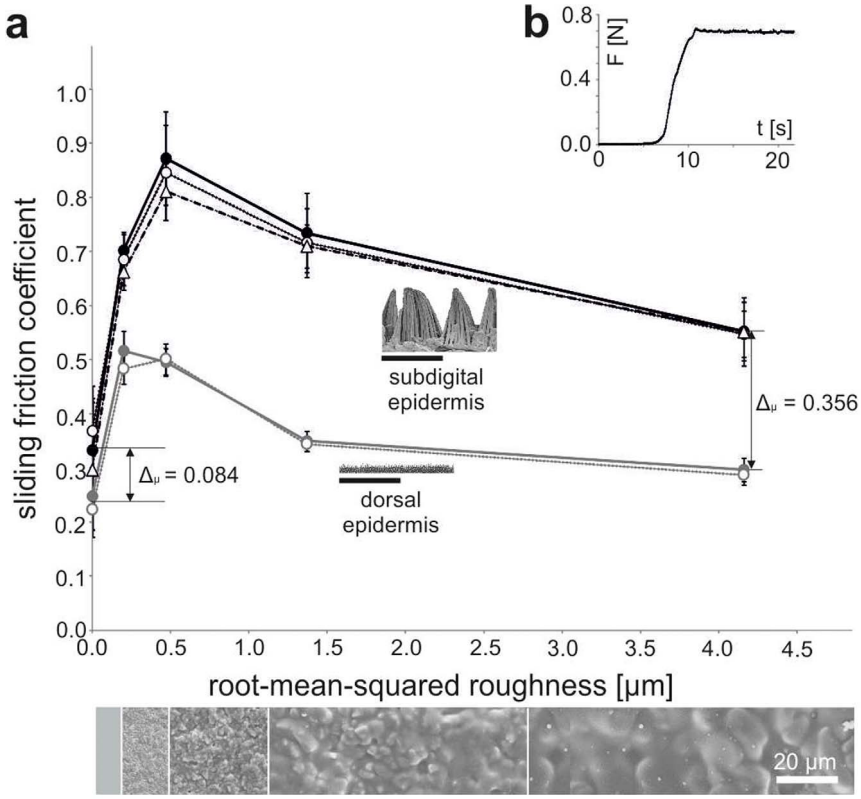

Figure 4 | Friction measurement. (a) Sliding friction coefficients of the subdigital epidermis (black) and the dorsal epidermis of the feet (gray) of anesthetized (N = 3) and dead individuals (N = 2) of *Ch. calyptratus* on glass (Rq = 0) and polish papers of different roughness (lower row of images shows scanning electron micrographs of corresponding surfaces). Sliding friction coefficients of the subdigital epidermis of anesthetized animals with a normal force of 589 mN are shown by a black solid line. Sliding friction coefficients of the subdigital epidermis of anesthetized animals with a normal force of 981 mN are shown by a black dotted line. Sliding friction coefficients of the subdigital epidermis of dead animals with a normal force of 569 mN are shown by a dashed black line. The solid and dotted gray lines show the sliding friction coefficients of the dorsal epidermis of the feet of anesthetized animal with normal force of 589 and 981 mN. Error bars represent the standard deviations of each five measurements of the two dead or three anesthetized individuals. Scale bars of scanning electron micrographs = 20 μm. On rough surface, the difference between subdigital epidermis and the dorsal epidermis of the feet is greater than on the smooth surface. (b) Single measurement of the friction force between the subdigital epidermis of the male individual and the substrate with 0.3 μm grain size (Rq = 0.2 μm) at a normal force of 981 mN. Sliding friction force increased after the system was set in motion and then motion was kept at constant speed. Static friction force (usually visible as a peak in the curve) was not observed.

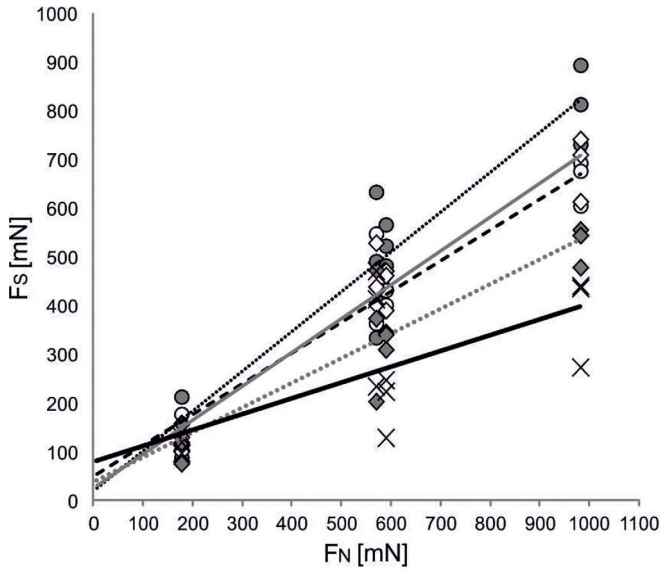

Figure 5 | Sliding friction forces measured on the subdigital epidermis of *Ch. calyptratus* under three different loads on the polish papers with 0.3 (white dots), 1 µm (gray dots), 3 (white dots), and 12 µm grain size (gray dots) and glass (black crosses). Each dot, rhomb and cross represents the mean value of five measurements. Sliding friction forces at 177 and 569 mN were measured in three dead individuals. Sliding friction forces at 589 and 981 mN were measured in three live individuals. In the measured range, sliding friction forces (Fs) were linear to normal forces (FN). Regression lines: 0.3 µm grain size (black dashed line): $y = 0.63x + 50$, $R = 0.914$; 1 µm grain size (black dotted line): $y = 0.82x + 21$, $R = 0.881$; 3 µm grain size (gray line): $y = 0.68x + 36$, $R = 0.929$; 12 µm grain size (gray dotted line): $y = 0.50x + 40$, $R = 0.811$; glass (black line): $y = 0.33x + 78$, $R = 0.487$.

(SD = 75.4), the effect of substrate type on friction force was quite high (SD = 78.09). Intercepts between the substrates were different from zero (glass = −83.3; 0.3 µm = 35.4; 1 µm = 112.8; 3 µm = 52.7; 12 µm = −39.7). The slope for the effect of normal forces on the friction forces was 0.612 (standard error = 0.0203, t value = 30.110, confidence interval 2.5% = 0.573, confidence interval 97.5% = 0.652).

Foot span in relation to the rod circumference. The male individual (T1) of *Ch. calyptratus* had a foot span of 31 mm. The two female individuals (T2 and T3) had foot spans of 29 and 25 mm respectively. The relation between the foot span and the rod circumferences is shown for all three individuals separately in percentage in Fig. 6. For example, one individual (T2) was able to encompass only 40% of the rod circumference of rods of 22 mm, but 90% of rods of 10 mm (Fig. 6 a). In cases where the circumference was smaller than the foot span, the animals were able to encompass more than 100%. For example, a rod of 6 mm diameter was encompassed up to 150% by the animal. In those cases the animals were not able to apply their claws for locomotion because they were not able to bring them into contact with the rod surface.

Table 1 | Surface parameters (mean ± standard deviation) of the substrates used in friction experiments (see Figs. 3, 4). All parameters, such as arithmetical mean roughness (Ra), root mean squared roughness (Rms), and the maximum profile valley depth (Rv), were measured with white light interferometry

substrate	Ra [µm]	Rms [µm]	Rv [µm]
polishing paper 0.3 µm	0.15 ± 0.01	0.20 ± 0.02	1.68 ± 0.48
polishing paper 1 µm	0.38 ± 0.05	0.47 ± 0.06	2.33 ± 0.29
polishing paper 3 µm	1.13 ± 0.28	1.37 ± 0.28	5.54 ± 1.08
polishing paper 12 µm	3.39 ± 1.02	4.16 ± 0.97	16.05 ± 1.79

Climbing performance. Observations of the climbing performance of three individuals of *Ch. calyptratus* on rods of two different materials, glass and wood, having different diameters showed that the animals' ability to climb depended on the material and the diameter of the rods (Fig. 6b). On thin rods of wood and glass, where the foot span was larger than the circumference, the animals were able to sit as well without using their claws as they were on thicker rods where they were able to apply their claws (rods that can be encompassed to more than 90%). On wood the holding ability decreased when the animals were able to encompass less than 50% of the circumference of the rods. The animal with the smallest foot span (T3) was not able to sit on horizontal rods with a diameter of 22 mm, whereas T2 as well as the animal with the largest foot span (T3) were still able to sit on this same rod having 30° and 90° inclination. On glass, the climbing ability of the animal with the smallest foot span (T3) still decreased at a rod diameter of 12 mm. The animal with the largest foot span was even able to sit on a 10° inclined rod of 16 mm diameter. T2 was unable to sit on any glass rod.

Discussion

Chameleon setae: friction enhancing function on a wide range of roughness. Friction measurements with the epidermis of *Ch. calyptratus* provided evidence of the friction increasing effect of subdigital setae in comparison to the spines on the dorsal sides of the chameleon feet. Sliding friction coefficients of the subdigital epidermis were significantly higher (up to 90%) than those of the upper sides of the feet on the polish paper surfaces. Also on glass significant differences were found at 981 mN normal force. Our results are consistent to the findings of a recent study by Khannoon et al.[43], where higher sliding friction was measured on subdigital scales in *Ch. calyptratus* in contact with a glass bead than on scales of the dorsal side of the feet. However, sliding friction of the subdigital epidermis on glass was in our study considerably higher ($\mu = 0.37$ under 981 mN normal force) than in the measurements of Khannoon et al.[43] ($\mu = 0.21$). This discrepancy could be due to different experimental setups. Khannoon et al.[43] measured friction with a glass sphere of 4 mm diameter over a sliding distance in the range of single scales which could cause non-uniform load distribution to scales and setae, whereas our study reflects the contribution of entire nominal contact area more corresponding to the situation on natural flat type of substrates during real locomotion. By the use of glass rods of similar diameter to plant twigs, which are the common substrate for chameleon locomotion, as substrates, and by applying normal force in a range that is generated by the animal body mass the contact geometry of scales, setae, and the substrate in our friction measurement may be assumed to be close to the real situation during locomotion. Since friction force is equal to the product of the normal force and the friction coefficient, due to the evolutionary transition from spines to setae, chameleons can save about one half of their muscle power (normal load) for generating same friction forces. Solely by the microornamentation of their subdigital pads, chameleons may be able to reduce their energetic costs for arboreal locomotion to a great extent.

Up to now the friction increasing function of subdigital microstructures of *Ch. calyptratus* was only investigated on glass surfaces. In nature, *Ch. calyptratus* climbs on a variety of different surface geometries. The chosen polish papers are only a selection of the wide range of substrate roughnesses in the natural habitat. Nevertheless, our study shows that the probably from spines evolved subdigital setae of *Ch. calyptratus* not only increase the friction on glass surfaces, but even to a greater extent on rough surfaces. Our linear mixed-effect analysis showed that substrate roughness significantly

Table 2 | Comparison of sliding friction coefficients of the live individuals of *Ch. calyptratus*. Median and percentiles (25%, 75%) of the friction measurements

epidermis, FN	glass	0.3 μm	1 μm	3 μm	12 μm
ventral, 589 mN	0.348 (0.224, 0.426)	0.703 (0.686, 0.733)	0.895 (0.793, 0.944)	0.762 (0.690, 0.785)	0.544 (0.510, 0.600)
ventral, 981 mN	0.409 (0.306, 0.434)	0.701 (0.651, 0.723)	0.880 (0.756, 0.919)	0.724 (0.652, 0.767)	0.570 (0.515, 0.577)
dorsal, 589 mN	0.248 (0.227, 0.268)	0.509 (0.496, 0.536)	0.491 (0.477, 0.521)	0.350 (0.332, 0.363)	0.308 (0.276, 0.314)
dorsal, 981 mN	0.226 (0.187, 0.261)	0.483 (0.465, 0.508)	0.508 (0.476, 0.517)	0.344 (0.338, 0.351)	0.291 (0.277, 0.300)

influences the friction forces. The highest friction coefficients of the subdigital epidermis were measured on polishing paper of 1 μm grain size, corresponding to a root-mean-square-roughness (Rq) of 0.47 μm. Since the material of all tested polish papers is the same, differences of frictional properties can be only addressed to the differences in the surface profile.

Role of claws and grasping feet in chameleon locomotion. Although our measurements provided evidence that *Ch. calyptratus* possesses effective epidermal structures on its feet increasing friction on a wide range of surface topographies, our experiments on the climbing performance on different rods showed that claws and muscle power are indispensable for locomotion. Our experiments on rods of different diameter and inclination demonstrated that, without muscle-generated normal forces, friction of the epidermis is not great enough to counteract the weight forces of animals. Our experimental animals could only sit and climb on thin rods of wood of which they could encompass 50% of the circumference. On these rods, animals were able to press their epidermal system onto the substrate surfaces using the opposite parts of their grasping feet. Our friction measurements under different load conditions, at a biologically relevant range, showed that friction forces of subdigital pads are proportional to normal forces over wide range of loads. By controlling the grasping forces chameleons can thereby control the amount of friction required for vertical locomotion. On thicker rods, with a larger circumference than the span of the chameleon's feet, animals were not able to bring both parts of their feet into a grasping position and to apply pressure. The difference in climbing ability was observed in the dependence on the rod material. This experiment demonstrated the high relevance of claws for chameleon locomotion on twigs. Whereas on wood, the animals best perform on rods of medium thickness (16 and 18 mm), on glass their climbing ability already decreased at a diameter of 12 mm. In grasping on curved substrates, the foot span is elongated by the length of claws. This allows the application of muscle power also on sticks of larger diameters. However, the effective application of claws requires either interlocking with surface asperities or pricking in the soft substrate. Both techniques can be applied on the soft rough wood but not on smooth rigid glass surface.

Chameleon vs. gecko: the mechanism of friction-enhancement. In lizards subdigital setae evolved convergently as an adaptation to arboreal locomotion and their shape is similar in Chamaeleonidae, Gekkota, Polychrotidae, and some Scincidae[1,10]. A comparison of the morphology and function of the subdigital system of *Ch. calyptratus* and the well-studied adhesive pads of *Gekko gecko* can contribute to the understanding of the friction increasing mechanism and functional priciple of chameleon setae. Up to now, van der Waals forces have been assumed to be the main physical mechanism for friction generation by lizard setae. As a result, maximization of the van der Waals forces was considered to be the evolutionary adaptation behind the spatula-like setal shape in arboreal lizards[7]. In order to provide maximal contact area resulting in an optimal use of van der Waals forces, the adhesive systems must be adaptable to the surface roughness at macro-, micro-, and nanoscale levels. In *G. gecko*, a large contact area between the substrate and the relatively stiff keratin of spatulae[45] is achieved by a hierarchical organization of the adhesive pad[31]. Their inclination makes setae adaptable to the microscale roughness due to their deflection ability[46]. Through thin terminal plates (spatulae), projecting in a certain direction[1,5,9,16,30], setae can also come into intimate contact even with a nanoscale substrate roughness[28,31]. Despite this good adaptability to the substrate in the subdigital system in geckos, measurements and behavioral studies revealed that both friction and adhesion are significantly reduced on a certain range of roughness[31,32]. Measurements of the pull-off forces of single spatulae of *G. gecko* on epoxy surface of different roughness showed a distinctive decrease of the pull off force between 100 and 300 nm RMS roughnesses[31]. These results are confirmed by locomotion experiments with this species on inclined surfaces[31]. Whereas animals firmly adhered to the ceiling on glass and polish papers with a nominal asperity size of 3, 9, and 12 μm, they started to slide on the slope of 135° on polish papers of 0.3 μm asperity size and slid off the substrate. On 1 μm asperity size they must continuously renew contact due to the decreased static friction[31]. In *Ch. calyptratus* we found exactly the opposite performance with low climbing ability and frictional coefficients on glass surface and the highest friction on the substrate with the asperity size of 1 μm. The reasons for the decreased attachment ability of *G. gecko* on certain profiles are well understood. The great effect of an even slight adjustment of size and shape of setal tips in animals was thoroughly discussed by Persson and Gorb[28]. The spatulae are presumably not able to adapt well to the surface asperities of similar dimensions and are thereby not close enough to generate attractive molecular interactions[31]. When

Table 3 | Kruskal-Wallis One Way ANOVA on ranks, (all substrates: $P \leq 0.001$, $DF = 3$) and pairwise multiple comparison (all substrates: Tukey Test, $P < 0.05$) of the sliding friction coefficients of the subdigital (ventral) and the dorsal epidermis of the feet at different normal forces (589 and 981 mN) on different substrates (glass, polish paper with 0.3, 1, 3, and 12 μm grain diameter). Asterisks indicate significant differences

	Glass	0.3 μm	1 μm	3 μm	12 μm
ventral 981 mN × dorsal 981 mN	5.825*	7.170*	6.209*	6.520*	6.949*
ventral 981 mN × dorsal 589 mN	4.302*	5.411*	6.520*	6.091*	6.106*
ventral 981 mN × ventral 589 mN	1.612	0.724	0.577	0.695	0.251
ventral 589 mN × dorsal 981 mN	4.214*	7.895*	6.786*	7.215*	7.200*
ventral 589 mN × dorsal 589 mN	2.691	6.136*	7.097*	6.786*	6.357*
dorsal 589 mN × dorsal 981 mN	1.523	1.759	0.310	0.429	0.843

Table 4 | Kruskal-Wallis One Way ANOVA on ranks, (589 mN: $P \leq 0.001$, $H = 64.458$, $DF = 4$; 981 mN: $P \leq 0.001$, $H = 63.890$, $DF = 4$) and pairwise multiple comparison (Tukey Test, $P < 0.05$) of the sliding friction coefficients of the subdigital epidermis on different substrates (glass, polish paper with 0.3, 1, 3, and 12 μm grain size). Asterisks indicate significant differences

substrate combination	589 mN: q value	981 mN: q value
glass × 0.3 μm	6.149*	6.362*
glass × 1 μm	10.248*	10.070*
glass × 3 μm	7.487*	7.547*
glass × 12 μm	2.772	2.677
0.3 μm × 1 μm	4.099*	3.708
0.3 μm × 3 μm	1.339	1.185
0.3 μm × 12 μm	3.376	3.632
1 μm × 3 μm	2.760	2.523
1 μm × 12 μm	7.475*	7.393*
3 μm × 12 μm	4.715*	4.869*

asperities have a size beyond this range, the surfaces on top of or the sides of single asperities are large enough that the entire spatula can come into contact[31]. However, the diminished attachment ability on certain surfaces does not necessarily lead to a total detachment of the system, as the adhesive systems of animals generate higher adhesive forces than the maximal pulling forces resulting from the body mass of the animals[26]. This relationship between the maximal forces that can be generated by the adhesive system and the animal weight is described by the "safety factor"[26]. If the safety factor is higher than 1, animals with adhesive structures may maintain their ability for locomotion on inclines, walls, and ceilings even when their adhesive system is partially damaged or contaminated, or when the contact with the substrate is reduced due to the presence of particular roughness.

At the first sight, setae of *Ch. calyptratus* lack morphological features that are responsible for the generation of high friction and adhesive forces in subdigital pads of *G. gecko*. SEM images of 17 chameleon species[36] show that their subdigital microstructures, especially the endings of setae, are oriented perpendicular to the underlying plane (isotropic geometry) and not declined as in *G. gecko* (anisotropic geometry). In chameleons, neither the setal stalks nor the tips are inclined in a certain direction[47]. In top-view, SEM images of chamaeleonid setal tips show no predefined bending direction, but can be bent to all directions equally. Instead of typical triangular *G. gecko* spatulae, setae of *Ch. calyptratus* have fine fibrous tips. How can these exceptional microstructures generate friction on a wide range of surface geometries? The cylindrical geometry of the fibrous tips of *Ch. calptratus* has more degrees of freedom for bending than the triangular spatula-like shape, which convergently evolved in the three other clades of arboreal lizards[1]. Fine fibrous tips enable greater contact with fine cavities of microroughness and this effect could explain the exceptional high friction on the substrate of 1 μm grain size (Fig. 7). On a smooth surface, the weak increase of friction of this type of setae, in comparison to rough surfaces and epidermal spines, can be explained by the reduced area of contact between the cylindrical cross-section of setal tips and the substrate. On smooth substrates triangular terminal plates (spatulae) of *G. gecko* generate much larger contact area and demonstrate very strong friction and friction-mediated adhesion.

The inclined setae of *G. gecko* have the advantage that setae become more adaptable, because leverage effects contribute to the deflection of setal stalks[47]. Also, the detachment process of nanoscale contacts becomes more controllable with inclined setae and oriented spatulae that occur in other lizards and arthropods[48–50]. The anisotropy in the arrangement of setae and spatulae makes the frictional and adhesive properties of the system direction dependent along the

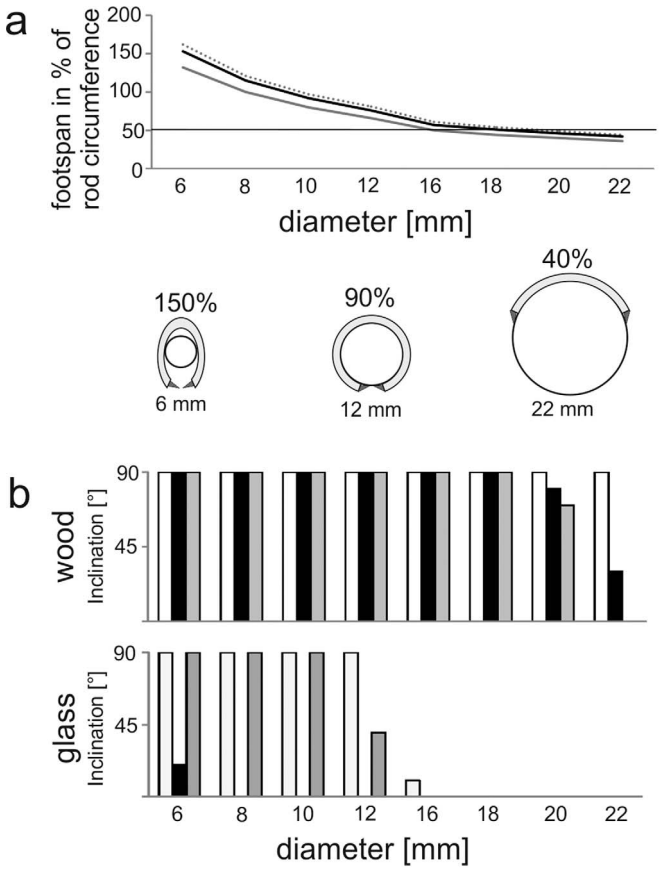

Figure 6 | Climbing performance of *Ch. calyptratus*. (a) Relationship between cylinder circumferences and the foot spans averaged from all four feet for the male (dotted line, T1) and the two female (black line T2, gray line T3) individuals of *Ch. calyptratus*. (b) Climbing performance of three individuals of *Ch. calyptratus* on rods of wood and glass of different diameters inclined in steps of 10°. Data of the male individual (T1) is shown with white bars. Black and gray bars show the climbing performance of the two females (T2 and T3).

longitudinal axis of the toe. In *G. gecko*, the highest friction is generated, when the tips of toes are pulled towards the center of the foot[25]. By splaying its toes, the gecko is able to adhere by its foot, although each single toe provides friction only in a single direction[27]. For this kind of locomotion, a sufficiently large and flat substrate is ideal. Through this principle, *G. gecko* is even able to climb onto overhangs, where the mass-related pulling force of the body is perpendicular to the surface[31]. Chameleons, on the contrary, are well adapted to their ecological niche, which is a three dimensional arrangement of twigs[37,41,51]. For locomotion on narrow perches, they have a long bendable grasping tail (except leaf-chameleons) and their toes are fused into pairs and triads forming prehensile feet[37]. By this morphology the ability to use the opposing toes is limited to one axis. However, similar to other arboreal lizards also chameleons need to withstand shear forces in all directions. Aligned setae, as in other pad-bearing arboreal lizards, providing friction mainly in one direction in combination with the grasping feet would not be suitable for this requirement in the case of chameleon pad geometry. To provide high friction in any direction, even though grasping feet and tail have a limited spatial mobility, subdigital, and subcaudal setae of chameleons are rather arranged isotropically and perpendicularly to the underlying surface of each scale and their fibrous tips are equally bendable in every direction[36]. Due to this morphology, subdigital setae of *Ch. calyptratus* have no anisotropy of frictional properties. With a glass bead Khannoon et al.[43] measured the same

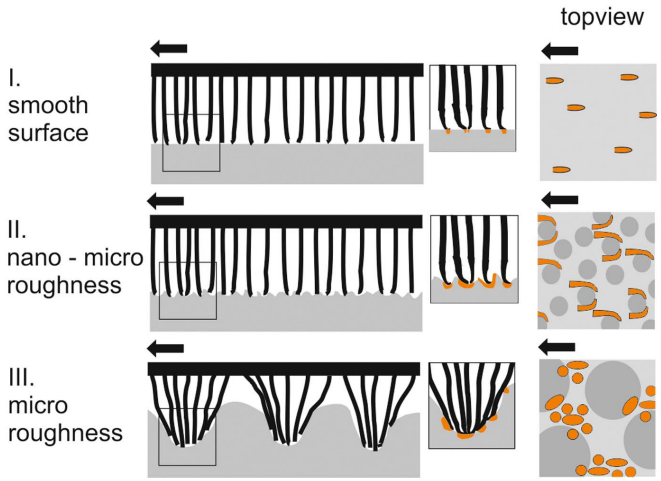

Figure 7 | Possible configuration of setae and their tips on the different surface topographies (I.–III.) during shear process in side and top views. The direction of movement is shown by arrows. The hypothetical areas of contact are marked orange. I. Due to the overall constant length of setae on smooth surfaces, only the fibrous tips are in contact with the substrate. II. On asperities from the nano scale up to few microns, fibrous setal tips have contact with the surface asperities. In comparison to smooth surfaces, the area of contact is larger here. Also effects of entanglement and interlocking can potentially occur. III. On rough surfaces at the micro scale, friction is mainly increased due to interlocking between whole setae and large surface asperities. Also clustering, which was often observed in subdigital setae (Spinner et al., 2013), does not necessarily decrease friction, but may even increase friction at certain dimensions/shape of surface asperities.

range of friction forces in all directions (lateral and proximal-distal) and at all locations of the subdigital pad (proximal, distal, medial).

How can *Ch. calyptratus* generate friction an a microscale roughness with its perpendicular setal stalks? Also on the rough surface of 12 μm grain size we measured significantly higher friction on the subdigital epidermis than on the dorsal sides of the feet. This effect could be explained, by interlocking at the micro and nanoscale. In our SEM and light microscopy images we revealed that setae were flexible enough to incline toward each other. In case of contact with surface structures of similar dimensions, these structures can indent arrays of setae (Fig. 7). Clustering, which was always considered to deminish attachment ability in seta-based biological adhesive systems[52,53], possibly may enhance such an "interlocking" of setal clusters with the microscale roughness (Fig. 7).

A further effect of chameleon setae is the prevention of stick-and-slip events. This means that in pulling, the fibrous chameleon setae similar to spatulate gecko setae[54] generate relatively constant dynamic friction rather than a set of stick-slip events. This geometry-based frictional effect was also demonstrated in artificial gecko-inspired adhesives[55]. Observations of the contacts of these synthetic surfaces in comparison to the flat samples made of the same materials indicate that the continuous sliding behaviour of fibrillar surfaces at the macroscale is a result of numerous randomly occurring stick-and-slip events at microscale[54,55].

Our study clearly shows the friction-increasing function of the setal pads in chameleons on a wide range of surface geometries. We demonstrated that friction forces increase proportionally to an increase of normal forces. From all tested surface geometries the highest friction was measured on the substrate of 1 μm grain size (Rq = 0.47 μm). That is why it can be assumed that despite to superficial resemblance of chameleon setae to the adhesive setae of geckos and anoles, the chamaeleonid subdigital microstructures have a different functional principle. Both the lack of spatulae and perpendicular arrangement of setae in *Ch. calyptratus* suggest rather an interlocking mechanism on micro and nano substrate asperities, whereas van der Waals forces, that are the basis for adhesion of *G. gecko*, play presumably a subordinated role. However, adhesive forces of chameleons on different substrates have to be characterized in further studies. In any case, our study shows that although the subdigital setae of *Ch. calyptratus* generate friction effectively, their friction is not high enough to enable locomotion on the flat substrates without additional generation of normal force. The firm grip on typical substrate curvatures additionally enhances the effect of the epidermal system of setae, which is well-coordinated with the claws and the grasping feet.

Methods

Frictional properties of the epidermis and climbing performance were examined in three individuals of *Chamaeleo calyptratus* DUMÉRIL & DUMÉRIL, 1851 (1 male, 2 females). Both experiments were performed in the course of one week after the animals finished their shedding process, in order to minimize the influence of contamination or epidermal damage on the measurements. The animals were purchased from a German breeder as juveniles and were kept in our institute (Institut für Zoologie, Rheinische Friedrich-Wilhelms-Universität Bonn, Germany). Additional measurements of the subdigital friction were done using three frozen individuals of *Ch. calyptratus*. The specimens were obtained from Prof. Dr. Wolfgang Böhme and Dr. Nicola Lutzmann (Forschungsmuseum Alexander Koenig, Bonn, Germany). Light microscopic images were taken from the skin of the frozen individuals.

Animal experiments. Experiments with living individuals of *Chamaeleon calyptratus* were approved by the Landesamt für Natur, Umwelt und Verbraucherschutz Nordrhein-Westfalen, Germany, under the number 84-02.04.2011.A401 and were in accordance with relevant guidelines and regulations.

Light microscopy. For light microscopy single subdigital scales were dissected from the frozen individuals of *Ch. calyptratus*. The samples were placed in (a drop of) water between a microscope slide and a cover slip and examined with a light microscope (Zeiss Axioplan with the camera Zeiss AxioCam MRc and the software Axio Vision (Carl Zeiss Microscopy GmbH, Jena, Germany).

Frictional measurements. Static and sliding friction were measured on all three individuals. The animals were anesthetized with an anesthetic vaporizer through a tube with 2% isoflurane (Delta Select, ActavisDtl. GmbH & Co KG, München, Germany) in carbogen gas (95% O_2 and 5% CO_2). Under the effect of isoflurane, one hind and one fore foot of each individual could be arranged on a tailored rigid foam board for the measurements. For friction measurement of the subdigital epidermis the animals lay on their back under the board. In this position one extended limb could be placed through a hole in the board so that the ventral sides of the open feet were at the top of the board (Fig. 3 a). For friction measurements of the dorsal epidermis of the feet the animals were laid on their side. This way the outer toes of the grasping feet of the upper hind- and forelimb could be placed on the board (Fig. 3 b). In both cases the hind- and forefoot were spaced at 8 cm. During the measurements, perpendicular needles pinned into the board, between the claws, prevented slipping of the feet.

For measuring friction different hollow cylinders with a diameter of 15 mm and a length of 20 cm were placed on the feet. The cylinders were connected with the bending beam of a force sensor (Kraftsensor S, LD Didactic, Hürth, Germany), using a silicon-PTFE tempered braided fishing line (Stroft GTP, Waku GmbH, Germany), movable in both directions parallel to the rods driven with a velocity of 1.5 m/h by an electric motor (Fig. 3 a). Data were recorded in intervals of 5 ms with the accompanying software CASSY lab 1 (LD Didactic, Hürth, Germany). Sliding force data were taken every 10 s from time-force curves as mean values of measured sliding forces. This time period corresponds to the distance of about 4 mm. One cylinder was out of glass (silicon dioxide). The other four steel cylinders were encased in polishing paper (aluminium (III) oxide, manufacturer information) having 0.3, 1, 3 and 12 μm grain size (FibrMet® Discs, Buehler, Illinois, USA). Both types of cylinders had a mass of 60 g and could be additionally loaded by inserting a steel rod having a mass of 40 g.

The friction forces between two surfaces also depend on the normal forces that press the surfaces against each other. In the experiment normal forces that press the substrates against the chameleon skin resulted from the weight of the rods. Using the mass of the rods and the gravitational force the normal forces in the experiment can be calculated. Since the rods were placed on both feet of the chameleons and both ends projected beyond the feet for the same length, it can be assumed that normal forces act equally strong on both feet. Using a gravitational acceleration of 9.81 m/s^2, these masses of the cylinders used correspond with normal forces of 589 and 981 mN that press the cylinders perpendicular to the epidermis. During the experiment, the order of cylinders used varied randomly. In this way, static and sliding friction between surfaces of different roughness and the subdigital areas of the hind and fore limb or the epidermis in the depression between the dorsal feet epidermis and antebrachium could be measured (Fig. 3).

Data for root-mean-squared roughness (Rq) of the polishing papers were determined by the Max-Planck-Institut für Intelligente Systeme Stuttgart (formerly Max-Planck-Institut für Metallforschung) using a white-light interferometer N.V.5000 5010s (Zygo Corporation, Middlefield, USA) and the software Metro Pro (version 7.10.0).

Static and sliding friction of each combination between the different substrates, subdigital epidermis and that of the antebrachium and the dorsal side of the feet was measured five times. The order of measurements was random. The experiments were conducted under room conditions (T = 20–24°C, relative humidity = 45–55%).

Sliding friction coefficients were determined using the equation $F_s = \mu_s F_N$[44] from the normal forces and the measured sliding forces. Frictional measurements in dead animals were done as described above, but with a cylinder mass of 18 and 58 g, corresponding with forces of 177 and 569 mN (applying a gravitational acceleration of 9.81 m/s^2). For this measurement only one foot was fixed. The other support was an additional glass cylinder (Fig. 3 c). Thus, sliding friction coefficients which were calculated from the measured sliding friction forces were only the mean from the two coefficients of both combinations of the support material, epidermis-glass and glass-glass. Since we also did frictional measurement of cylinders laying on two glass supports, we were able to subtract the influence of the glass support for comparison of data from this experiment with those of the live animals.

Data were also analyzed with a linear mixed effect model. Linear mixed effect analysis was performed with R (R Development Core Team) and lme4 (Bates et al., 2012) software. The normal load was considered as fixed effect. Substrates and individuals in repeated measurements were considered as random effects.

Climbing performance. Climbing performance of all three individuals was observed using 50 cm long rods of glass and wood having different diameters (6, 8, 10, 12, 16, 18, 20 and 22 mm). The animals were placed on the horizontal oriented rods. In cases, when the animals were able to sit, the rods were further tilted manually by 10° and then fixed. Measurement was discontinued at inclination angles that caused the animals to slide. Trails in which the angle of inclination was such that the animals were repeatedly not able to sit were considered as failed. Trails in which the chameleon's belly or tail touched the rod were not used. Trails were then repeated. Foot spans of the animals were measured from photos with the free software Image J 1.45 and averaged for all four feet of the individuals. At the time of testing the body mass of the male individual (T1) was 74 g and that of the females (T2, T3) was 80 g and 58 g respectively.

1. Williams, E. E. & Peterson, J. A. Convergent and alternative designs in the digital adhesive pads of scincid lizards. *Science* **215**, 1509–1511 (1982).
2. Beutel, R. G. & Gorb, S. N. Ultrastructure of attachment specializations of hexapods (Arthropoda): evolutionary patterns inferred from a revised ordinal phylogeny. *J. Zool Syst. Evol. Res.* **39**, 177–207 (2001).
3. Rovner, J. S. Adhesive hairs in spiders: behavioral functions and hydraulically mediated movement. *Symp. Zool. Soc. Lond.* **42**, 99–108 (1978).
4. Coddington, J. A. & Levi, H. W. Systematics and evolution of spiders (Araneae). *Annu. Rev. Ecol. Evol. Syst.* **22**, 565–592 (1991).
5. Irschick, D. J. *et al.* A comparative analysis of clinging ability among pad-bearing lizards. *Biol. J. Linn. Soc.* **59**, 21–35 (1996).
6. Stork, N. E. A comparison of the adhesive setae on the feet of lizards and arthropods. *J. Nat. Hist.* **17**, 829–835 (1983).
7. Arzt, E., Gorb, R. & Spolenak, R. From micro to nano contacts in biological attachment devices. *Proc. Natl. Acad. Sci.* **100**, 10603–10606 (2003).
8. Peattie, A. M. & Full, R. J. Phylogenetic analysis of the scaling of wet and dry biological fibrillar adhesives. *Proc. Natl. Acad. Sci.* **104**, 18595–18600 (2007).
9. Hiller, U. Untersuchungen zum Feinbau und zur Funktion der Haftborsten von Reptilien. *Z. Morphol. Tiere* **62**, 307–362 (1968).
10. Ruibal, R. & Ernst, V. The structure of the digital setae of lizards. *J. Morphol.* **117**, 271–294 (1965).
11. Gorb, S. N. *Attachment Devices of Insect Cuticle* (Kluwer, Dordrecht, The Netherlands, 2001).
12. Peterson, J. A. The evolution of the subdigital pad of anolis 2. Comparisons among the iguanid genera related to the anolines and a view from outside the radiation. *J. Herpetol.* **17**, 371–397 (1983).
13. Bauer, A. M. & Good, D. A. Scaling of scansorial area in the genus *Gekko*. In *Studies in Herpetology* (Karls-Universität, Prag, 1986).
14. Bauer, A. M. Morphology of the adhesive tail tips of carphodactyline geckos (Reptilia: Diplodactylidae). *J. Morphol.* **235**, 41–58 (1998).
15. Peattie, A. M. Subdigital setae of narrow-toed geckos, including a eublepharid (*Aeluroscalabotes felinus*). *Anat. Rec.* **291**, 869–875 (2008).
16. Dellit, W. D. Zur Anatomie und Physiologie der Geckozehe. *Jenaische Zeitschrift für Naturwissenschaft* **68**, 613–656 (1934).
17. Maderson, P. F. A. Keratinized epidermal derivatives as an aid to climbing in gekkonid lizards. *Nature* **203**, 780–781 (1964).
18. Rizzo, N. W. *et al.* Characterization of the structure and composition of gecko adhesive setae. *J. R. Soc. Interface* **3**, 441–451 (2006).
19. Russell, A. P., Johnson, M. K. & Delannoy, S. M. Insights from studies of gecko-inspired adhesion and their impact on our understanding of the evolution of the gekkotan adhesive system. *J. Adhes. Sci. Technol.* **21**, 1119–1143 (2007).
20. Gorb, S. N. The design of the fly adhesive pad: distal tenent setae are adapted to the delivery of an adhesive secretion. *Proc. R. Soc. B.* **265**, 747–752 (1998).
21. Voetsch, W. *et al.* Chemical composition of the attachment pad secretion of the locust *Locusta migratoria*. *Insect Biochem. Molec.* **32**, 1605–1613 (2002).
22. Federle, W., Riehle, M., Curtis, A. S. G. & Full, R. J. An integrative study of insect adhesion: mechanics and wet adhesion of pretarsal pads in ants. *Integr. Comp. Biol.* **42**, 1100–1106 (2002).
23. Betz, O. From nature to technical and medical application. Adhesive exocrine glands in insects: morphology, ultrastructure, and adhesive secretion. In *Biological adhesive systems* (Springer, New York, 2010).
24. Autumn, K. *et al.* Evidence for van der Waals adhesion in gecko setae. *Proc. Natl. Acad. Sci.* **99**, 12252–12256 (2002).
25. Autumn, K. *et al.* Adhesive force of a single gecko foot-hair. *Nature* **405**, 681–685 (2000).
26. Autumn, K. & Peattie, A. M. Mechanisms of adhesion in geckos. *Integr. Comp. Biol.* **42**, 1081–1090 (2002).
27. Autumn, K., Dittmore, A. Santos, D., Spenko, M. & Cutkosky, M. Frictional adhesion: a new angle on gecko attachment. *J. Exp. Biol.* **209**, 3569–3579 (2006).
28. Persson, B. N. J. & Gorb, S. The effect of surface roughness on the adhesion of elastic plates with application to biological systems. *J. Chem. Phys.* **119**, 11437–11444 (2003).
29. Huber, G. *et al.* Evidence for capillarity contributions to gecko adhesion from single spatula nanomechanical measurements. *Proc. Natl. Acad. Sci.* **102**, 16293–16296 (2005).
30. Huber, G., Gorb, S. N., Spolenak, R. & Arzt, E. Resolving the nanoscale adhesion of individual gecko spatulae by atomic force microscopy. *Biol. Lett.* **1**, 2–4 (2005).
31. Huber, G., Gorb, S. N., Hosoda, N., Spolenak, R. & Arzt, E. Influence of surface roughness on gecko adhesion. *Acta Biomater.* **3**, 607–610 (2007).
32. Pugno, N. M. & Lepore, E. Observation of optimal gecko's adhesion on nanorough surfaces. *BioSystems* **94**, 218–222 (2008).
33. Schleich, H. H. & Kästle, W. Ultrastrukturen der Zehenunterseiten einiger arborikoler Iguaniden. *Spixiana* **8**, 251–258 (1985).
34. Schleich, H. H. & Kästle, W. Hautstrukturen als Kletteranpassungen bei *Chamaeleo* und *Cophotis* (Reptilia: Sauria: Chamaeleonidae, Agamidae). *Salamandra* **15**, 95–100 (1979).
35. Müller, R. & Hildenhagen, T. Untersuchungen zu Subdigital- und Subkaudalstrukturen bei Chamäleons (Sauria: Chamaeleonidae). *Sauria* **31**, 41–54 (2009).
36. Spinner, M., Westhoff, G. & Gorb, S. N. Subdigital and subcaudal microornamentation in Chamaeleonidae: a comparative study. *J. Morphol.* **274**, 713–723 (2013).
37. Gans, C. The chameleon. *Natural History* **76**, 52–59 (1967).
38. Necas, P. *Chamäleons. Bunte Juwelen der Natur.* (Edition Chimaira, Frankfurt/M 1999).
39. Ruibal, R. The ultrastructure of the surface of lizard scales. *Copeia* **4**, 698–703 (1968).
40. Irish, F. J., Williams, E. E. & Seeling, F. Scanning electron microscopy of changes in epidermal structure occuring during the shedding cycle in squamate reptiles. *J. Morphol.* **197**, 105–126 (1988).
41. Fischer, M. S., Krause, C. & Lilje, K. E. Evolution of chameleon locomotion, or how to become arboreal as a reptile. *Zoology* **113**, 67–74 (2010).
42. Herrel, A. *et al.* Slow but tenacious: an analysis of running and gripping performance in chameleons. *J. Exp. Biol.* **216**, 1025–1030 (2013).
43. Khannoon, E. R., Endlein, T., Russell, A. P. & Autumn, K. Experimental evidence for friction-enhancing integumentary modifictions of chameleons and associated functional and evolutionary implications. *Proc. R. Soc. B* **281**, 20132334 (2014).
44. Tipler, P. A. & Mosca, G. *Physics for scientists and engineers.* (Palgrave Macmillan, 2008).
45. Peattie, A. M., Majidi, C., Corder, A. & Full, R. J. Ancestrally high elastic modulus of gecko setal beta-keratin. *J. R. Soc. Interface* **4**, 1071–1076 (2007).
46. Creton, C. & Gorb, S. Sticky feet: from animals to materials. *M. R. S. Bull.* **32**, 466–472 (2007).
47. Jeong, H. E., Lee, J. K., Kwak, M. K., Moon, S. H. & Suh, K. Y. Effect of leaning angle of gecko-inspired slanted polymer nanohairs on dry adhesion. *Applied Physics Letters* **96**, 043704–043704 (2010).
48. Tian, Y. *et al.* Adhesion and friction in gecko toe attachment and detachment. *Proc. Natl. Acad. Sci.* **103**, 19320–19325 (2006).
49. Pesika, N. S. *et al.* Peel-zone model of tape peeling based on the gecko adhesive system. *J. Adhesion* **83**, 383–401 (2007).
50. Varenberg, M., Murarash, B., Kligerman, Y. & Gorb, S. N. Geometry-controlled adhesion: revisiting the contact splitting hypothesis. *Appl. Phys. A - Mater.* **103**, 933–938 (2011).
51. Losos, J. B., Walton, B. M. & Bennett, A. F. Trade-offs between sprinting and clinging ability in Kenyan chameleons. *Functional Ecology* **7**, 281–286 (1993).
52. Jagota, A. & Bennison, S. J. Mechanics of adhesion through a fibrillar microstructure. *Integr. Comp. Biol.* **42**, 1140–1145 (2002).
53. Spolenak, R., Gorb, S. & Arzt, E. Adhesion design maps for bio-inspired attachment systems. *Acta Biomater.* **1**, 5–13 (2005).
54. Varenberg, M. & Gorb, S. Shearing of fibrillar adhesive microstructure: friction and shear-related changes on pull-off force. *J. R. Soc. Interface* **4**, 721–725 (2007).
55. Gravish, N. *et al.* Rate-dependent frictional adhesion on natural and synthetic gecko setae. *J. R. Soc. Interface* **7**, 259–269 (2010).

Acknowledgments

We thank Prof. Dr. Horst Bleckmann (Rheinische Friedrich-Wilhelms-Universität Bonn, Germany) and Dr. Tobias Kohl (Technische Universität München) for their advice and assistance in the anesthesia and for supporting this study. This work was supported by the

German Science Foundation (DFG, Graduiertenkolleg BIONIK) to G.W. and by the DFG grant GO10-1 to S.G.

Author contributions

M.S., G.W. and S.N.G. designed the experiments. M.S. conducted the experiments and wrote the main text of the manuscript. G.W. and S.N.G. contributed to various parts of the manuscript, especially to the discussion of results. S.N.G. provided corrections of all versions of the manuscript.

Additional information

Competing financial interests: The authors declare no competing financial interests.

How to cite this article: Spinner, M., Westhoff, G. & Gorb, S.N. Subdigital setae of chameleon feet: Friction-enhancing microstructures for a wide range of substrate roughness. *Sci. Rep.* **4**, 5481; DOI:10.1038/srep05481 (2014).